JZUS

Assessment of the phase synchronization effect in
modal testing during operation[*]

Zhi Chao ONG[†1], Hong Cheet LIM[1], Shin Yee KHOO[1], Zubaidah ISMAIL[2],

Keen Kuan KONG[1], Abdul Ghaffar Abdul RAHMAN[3]

(*[1]Department of Mechanical Engineering, Faculty of Engineering, University of Malaya, Kuala Lumpur 50603, Malaysia*)
(*[2]Department of Civil Engineering, Faculty of Engineering, University of Malaya, Kuala Lumpur 50603, Malaysia*)
(*[3]Faculty of Mechanical Engineering, University Malaysia Pahang, Pekan, Pahang Darul Makmur 26600, Malaysia*)
[†]E-mail: zhichao83@gmail.com; alexongzc@um.edu.my

Abstract: The impact-synchronous modal analysis (ISMA), which uses impact-synchronous time averaging (ISTA), allows modal testing to be performed during operation. ISTA is effective in filtering out the non-synchronous cyclic load component, its harmonics, and noises. However, it was found that at operating speeds that coincide with the natural modes, ISMA would require a high number of impacts to determine the dynamic characteristics of the system. This finding has subsequently reduced the effectiveness and practicality of ISMA. Preservation of signatures during ISTA depends on the consistency of their phase angles on every time block but not necessarily on their frequencies. Thus, the effect of phase angles with respect to impact is seen to be a very important parameter when performing ISMA on structures with dominant periodic responses due to cyclic load and ambient excitation. The responses from unaccounted forces that contain even the same frequency as that contained in the response due to impact are diminished with the least number of impacts when the phase of the periodic responses is not consistent with the impact signature for every impact applied. The assessment showed that a small number of averages are sufficient to eliminate the non-synchronous components with 98.48% improvement on simulation and 95.22% improvement on experimental modal testing when the phase angles with respect to impact are not consistent for every impact applied.

Key words: Experimental modal analysis; Vibration; Impact-synchronous modal analysis (ISMA); Impact-synchronous time averaging (ISTA); Modal testing; Phase synchronization
http://dx.doi.org/10.1631/jzus.A1600003   **CLC number:** O32

1 Introduction

Modal analysis is used in investigating the dynamic behavior of systems. This study enables an enhanced understanding and identification of the root cause of the vibration phenomena encountered in engineering by describing a system with its modal parameters, namely the natural frequencies, natural damping, and natural modes (Rossmann, 1999; Wang *et al.*, 2010a). These three parameters comprehensively define the dynamic characteristics of a system. Currently, there are two techniques used to extract these parameters, i.e., the classical experimental modal analysis (EMA) and operational modal analysis (OMA).

EMA has attracted attention and grown rapidly in popularity since the advent of the digital fast Fourier transform (FFT) analyzer in the early 1970s. In the modal data acquisition stage of EMA, the responses of a linear, time-invariant system are measured along with a known excitation, often out of its

normal service environment. This process normally takes place in a closely controlled condition, where the test structure is artificially excited by using either an impact hammer, or one or more shakers driven by broadband signals. Performing FFT on the measured signal will yield the frequency response functions (FRFs). FRFs are subjected to a range of modal identification algorithms, e.g., the complex exponential algorithm (CEA), least squares complex exponential (LSCE), Ibrahim time domain (ITD), and eigensystem realization algorithm (ERA), in an attempt to find the mathematical model which provides the closest description of the actually observed response by the system. Common applications of EMA include troubleshooting, structural modification, sensitivity analysis, structural health monitoring, structural damage detection, etc. (Dilena and Morassi, 2004; Guo et al., 2005; Fayyadh et al., 2011; Ismail, 2012; Ismail et al., 2012; Li et al., 2012; Garcia-Perez et al., 2013). However, conventional EMA has limitations: (1) simplified rather than exact boundary conditions of the system in a real situation are simulated in laboratory testing; (2) FRFs or impulse response functions (IRFs) are hard to measure in practice, especially on large and complex systems; (3) it requires the system to be in a complete shutdown state, which means no unaccounted excitation force will be induced into the system. In industrial applications, especially in petrochemical plants, the downtime cost is crucial and thus it is not practical to shut down the machinery under testing to perform EMA.

While EMA has been used successfully for many systems, it is difficult to perform on large and highly complex civil structures (e.g., buildings and bridges) as it is very difficult to excite the structure artificially. In addition, in some practical situations where the system cannot be shut down completely, OMA is preferred. In OMA, modal parameters are extracted based on the output responses measured without the input excitation information. Thus, it is important for the input excitation to have sufficient energy to excite all the modes of interest. The natural excitation applies on the structure can range from traffic load, wind, earthquake waves, to ambient vibration (He and Fu, 2001; Brincker and Ventura, 2015). Major developments of modal parameter identification algorithms are available both in the time and frequency domains, i.e., frequency domain decomposition (FDD), output-only least-squares complex frequency (LSCF) domain methods, natural excitation technique (NExT), auto-regressive and moving average vector (ARMAV) model, modified Ibrahim time domain (MITD), stochastic realization-based identification, and stochastic subspace-based identification (SSI) (James et al., 1995; van Overschee and de Moor, 1996; Guillaume et al., 1998; Brincker et al., 2000; Bodeux and Golinval, 2001; Lardies and Larbi, 2001).

Recently, there has been an upsurge in using OMA on long-span bridges to complement static testing and traditional visual inspection to locate promptly the presence of critical defects. This non-destructive testing provides detailed information for safety assessments, i.e., vibration-based structural health monitoring (SHM) on long-span bridges under extreme loads exemplified by the Run Yang, Tsing Ma, and Sutong Yangtze River bridges (Wong, 2004; Ding et al., 2008; Li et al., 2010; Magalhães et al., 2012; Wang et al., 2016). Unlike EMA, OMA is performed where the excitation and boundary conditions of the system are those seen during operation. It is therefore a valuable tool to replace EMA in the validation and updating of developed finite element models (Ding and Li, 2008; Wang et al., 2010b).

However, the lack of knowledge of the input forces does affect the parameters extracted. Mode shapes obtained from OMA cannot be normalized accurately, which affects the development of mathematical models thereafter. Besides, most OMA methods require random excitation with spectral energy varying slowly with the frequency (ideally, white noise excitation). In process equipment, the excitation can have strong periodic components, resulting in a forced periodic response. Most OMA methods are not able to distinguish between spectral peaks due to the forced harmonic vibration and those due to the resonant response of broadband excitation. For these reasons, OMA cannot be effectively applied for this application in general. Nevertheless, recent findings by a few researchers in the effort to improve the accuracy of modal extraction techniques are noted. A combination of mode shapes identified by OMA and a mass matrix of a finite element model in scaling of mode shapes was found in Aenlle and Brincker (2013). In Le and Argoul (2015), mother

wavelet was used as a filter in time-frequency domain decomposition (TFDD) and provided information in a narrow band around a cyclic load component or a natural mode. Thus, an indicator based on the kurtosis value and histogram was derived, which allows the recognition of a natural mode or a cyclic load component. Besides, a Gauss-Newton fitting algorithm was introduced in Bienert *et al.* (2015) to find the reduced least squares fitting of the experimental data to a harmonic deterministic function. This approach subtracts the cyclic load component from the raw time signal. However, information on the accuracy of modal parameter identification after the subtraction of the cyclic load component was not presented.

A novel method, named impact-synchronous modal analysis (ISMA), which uses impact-synchronous time averaging (ISTA) was proposed (Rahman *et al.*, 2011a; 2011b; 2014). This modal analysis technique focuses on the digital signal processing upstream of the collected data rather than the modal identification algorithm. In the commonly used time domain synchronous averaging technique, signal acquisition from a rotating machine is triggered at the same rotational position of the shaft using a tachometer for every cycle. The time block, i.e., the block of vibration data captured in time series of averaged signals, eliminates all the non-synchronous and random components, leaving behind only components that are integer multiples of the running speed. In ISMA, the same and simple averaging concept is used but only to achieve the reverse, i.e., to filter out all the speed synchronous and random signatures. It is effective in filtering out the cyclic load component, the harmonics, and noises, which are non-synchronous with the impacts. ISMA has the advantages of the OMA and EMA combined. It carries out the analysis while the system is in operation, and at the same time it is able to provide the actual input forces in the transfer functions, thus allowing for better modal extractions and mathematical model development. This novel technique has been successfully applied in both rotor and structural dynamic systems to determine the dynamic characteristics of structures without disturbing operations (Rahman *et al.*, 2011a; 2011b).

Previous research experimentally demonstrated that the number of averages or impacts had a very important effect when applying ISMA on structures with dominant periodic responses of cyclic loads and ambient excitation (Rahman *et al.*, 2014). However, it was found that at operating speeds that coincided with the natural modes, ISMA with random impacts required a high number of impacts to determine the dynamic characteristics of the system. This is probably due to the lack of information of phase angles with respect to impact and it has subsequently reduced the effectiveness and practicality of ISMA.

In this study, the effect of phase synchronization in ISMA during operation is investigated in simulation and experimental testing in the effort to enhance the effectiveness of the technique. The study looks into two conditions, i.e., consistent and inconsistent phase conditions, between the response due to impacts and the response from the cyclic load component. The effect on the FRF estimation is then studied.

2 Mathematical model

In ISTA, a series of time blocks, each triggered by an impact force signal, use the fact that all other responses are non-synchronous with the impacts. The time averaging of n blocks would result in eliminating all these non-synchronous components, leaving behind only the structure's response due to impacts. The effect of the phase angle with respect to impact in ISTA can be described as follows.

The sinusoidal signature is given by

$$y(t)=A\sin(\omega t+\beta)=a\cos(\omega t)+b\sin(\omega t), \qquad (1)$$

where A is the amplitude of the signature, ω the angular frequency (or cyclic load frequency), and β the phase angle. When $y(t)$ is captured in each individual block of time series at different β, the values a and b are different for each individual block of time series even though the amplitude A does not change corresponding to that individual block of time series. However, block averaging of this time series, i.e., all the individual blocks captured, will result in values of a and b diminishing to zero, subsequently reducing A to zero as well. To keep a and b consistent, $y(t)$ has to start at the same point for every block captured; i.e., β has to be consistent.

In the event of performing modal testing during operation, the total time response, $y(t)$, is captured in a time block with respect to a specific trigger condition (often the magnitude or slope of the excitation) (Phillips and Allemang, 2003). The $y(t)$ measured consists of two types of signals, i.e., $x(t)$ and $e(t)$, as follows:

$$y(t) = x(t) + e(t)$$
$$= \sum_{r=1}^{n} A_r e^{-\sigma_r t} \sin(\omega_{\mathrm{d}r} t + \beta_1) + R_2 \sin(\omega t + \beta_2), \quad (2)$$

where $x(t)$, a desired deterministic response signal due to impact consisting of the summation of all the modes r, is synchronous with every impact force applied, and $e(t)$ is the summation of the undesired deterministic signal of the periodic response of cyclic load with frequency of ω in addition with random ambient noises. Parameter σ_r is the decay rate, $\omega_{\mathrm{d}r}$ is the modal frequency, n is the maximum number of modes, A_r is the amplitude of mode r for the desired deterministic response signal due to impact, R_2 is the amplitude of the undesired deterministic signal of the periodic response of cyclic load, β_1 is the phase of the desired deterministic response signal due to impact, and β_2 is the phase of the undesired deterministic signal of the periodic response of cyclic load.

Eq. (2) can be written as

$$y(t) = \sum_{r=1}^{n} e^{-\sigma_r t} \left[a_r \cos(\omega_{\mathrm{d}r} t) + b_r \sin(\omega_{\mathrm{d}r} t) \right]$$
$$+ f_1 \cos(\omega t) + g_1 \sin(\omega t). \quad (3)$$

Signal $x(t)$ is triggered consistently with the impact force and is thus synchronous with phase β_1 in a time block (i.e., 4096 samples). Small variations in a_r and b_r would average to amplitude A_r in block averaging. However, the periodic response of cyclic load and random ambient noises, $e(t)$, is non-synchronous with every impact force applied, causing the phase value of β_2 to change for every individual block of time series captured and thus leading to different values of f_1 and g_1 corresponding to that individual block of time series. Because the values of f_1 and g_1 keep changing in all individual blocks, performing block averaging on all the individual

blocks captured in a time domain tends to diminish these non-synchronous components, i.e., f_1 and g_1, and subsequently reduces R_2 to zero as well. In short, performing ISTA on the total response signal $y(t)$ will filter out the signal $e(t)$, and the desired signal $x(t)$ will reinforce for every time block recorded over time. Note that this is similar to the response due to the impact signal obtained in modal testing during a stationary condition. It is worth mentioning that the cyclic load component can still be filtered out even if the cyclic load frequency (ω) equals one of the modal frequencies ($\omega_{\mathrm{d}r}$). In summary, preservation of signatures during time averaging depends on the consistency of their phase angles (β) on every time block but not necessarily on their angular frequencies (ω) (Timoshenko, 1974; Maia and Silva, 1997).

3 Experimental procedure

3.1 Virtual instrument simulation

When performing modal testing during operation, the response due to cyclic load (i.e., a periodical signal) and any ambient noise present themselves together with the response due to impacts. These unaccounted forces are filtered out in ISMA to give better results. To simulate and represent the actual scenario, we focus only on a periodical signal. We show that the phase angle with respect to impacts is one of the important parameters in getting rid of the disturbance from the periodical signal.

The phase angle of the dominant periodic responses due to cyclic load should be avoided to be consistent with every impact applied to enhance the effectiveness of ISMA. To study the effect of phase synchronization in ISMA, virtual instrument (DASYLab) was used to simulate the required conditions, which are difficult to achieve with the existing manually operated impact hammer.

In this assessment, the responses due to consistent impacts were first designed to be consistent with the periodic responses due to cyclic load for every impact applied (Fig. 1). Both responses contain the same frequency at 20 Hz. Meanwhile, in another simulation, consistent impacts were simulated, where the impacts applied were designed to be in the same frequency, i.e., 20 Hz, but at inconsistent phase angles with the periodic response due to cyclic

load (Fig. 2). The phase angles of the response generated by each impact are not consistent with the phase angles of the response due to cyclic load. Responses due to impact and responses due to cyclic load and noise are linearly superimposed to simulate the actual scenario when performing modal testing during operation. When performing ISMA in a real practice, the unaccounted force components can be
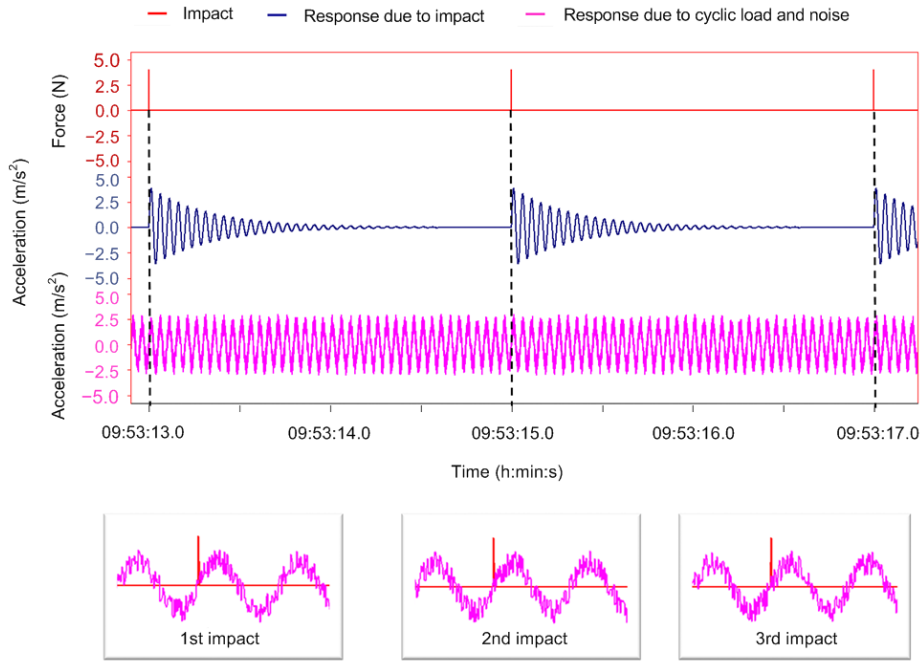

Fig. 1 Consistent phases with respect to every impact applied (for interpretation of the references to color in this figure legend, the reader is referred to the web version of this article)
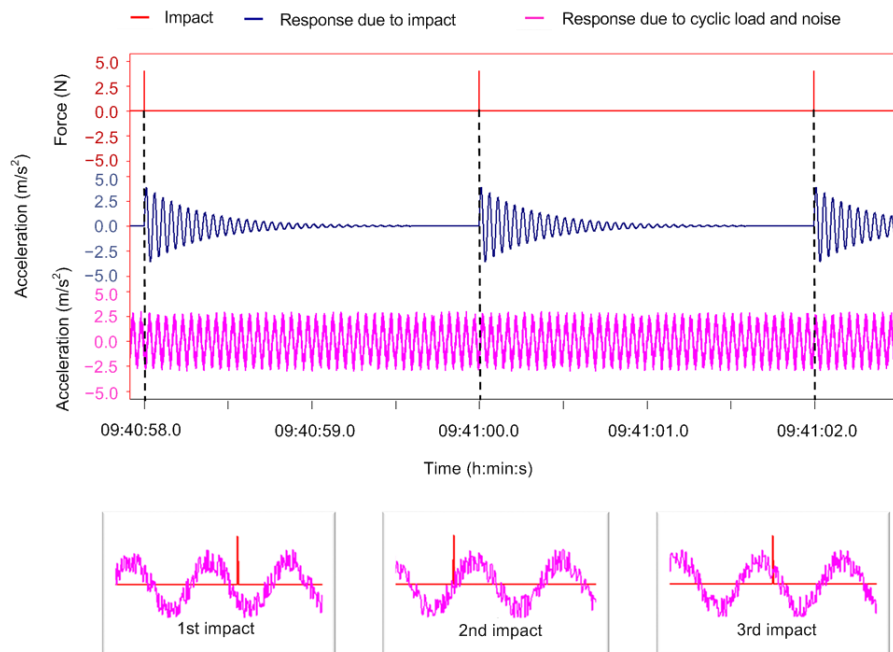

Fig. 2 Inconsistent phases with respect to every impact applied (for interpretation of the references to color in this figure legend, the reader is referred to the web version of this article)

more dominant than the response due to impact. Thus, it is essential to use exponential windowing in performing the dual task as it can (1) eliminate or minimize leakage due to truncated response signal on a lightly damped structure and (2) filter out all the responses contributed by the unaccounted forces, i.e., the cyclic load component in a time block. In the simulation, an exponential windowing function with a decay rate of 3 rad/s was applied to minimize leakage due to truncated response signal and to attenuate signals of a non-synchronous cyclic load component with respect to the impact, the harmonics, and noises to zero at the end of each time record window block as in real conditions. The effect of phase synchronization in ISMA is studied and evaluated by comparing both the time and frequency responses of the averaged superimposed responses with the benchmarked response due to impact. Note that the reduction of frequency response magnitudes at the first and second natural peaks and the cyclic load component are defined by the percentage of improvement.

3.2 Experimental modal testing

The assessment of the phase synchronization effect in modal testing during operation was performed on a laboratory motor-driven structure (Fig. 3) at 20 Hz with four averages. The block size and sampling rate used were 4096 samples and 2048 samples/s, respectively. This yields a data acquisition time of 2 s and a frequency resolution of 0.5 Hz. Data were obtained by using a data acquisition system together with an impact hammer exciting the point of interest (i.e., point 2 in Fig. 3), and an accelerometer was used to measure the response due to impact. ISTA was used to filter out the non-synchronous disturbances, which were the responses due to cyclic load and extraneous noise. The acquired time signals, i.e., impact forces and responses due to impacts, were then post-processed in ME'scopeVES to generate an FRF estimation. The FRF's estimation for operation at 20 Hz was presented in four scenarios: (1) consistent phase condition for all impacts, (2) consistent phase condition for certain impacts, (3) inconsistent phase condition for all impacts (ideal case), and (4) inconsistent phase condition for all impacts. Note that scenarios 2 and 4 are commonly obtained when a manual impact hammer is used. FRF estimation for a complete shutdown of the system was used as the

benchmark data. The estimated FRFs were than compared for both consistent and inconsistent phase conditions with the benchmark data, in order to evaluate the effect of phase synchronization in modal testing during operation.
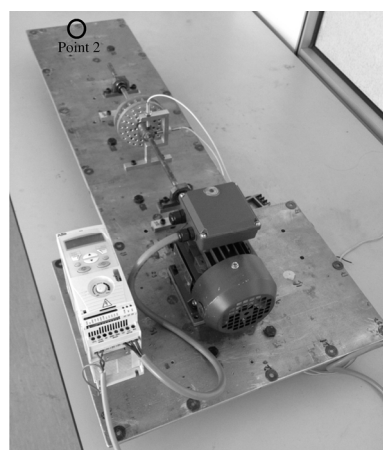

Fig. 3 Motor-driven test rig

4 Validation results and discussion

4.1 Simulation

4.1.1 Consistent phase condition

In the first simulation, the phase of response due to impacts is designed to be consistent with the phase of response due to cyclic load in every impact applied. Because of phase synchronization, the unaccounted force components which contain the same frequency as the response due to impacts are dominant and could not be filtered out. In this case, only the noises are eliminated after 30 averages. The linear superimposition of response due to impact and periodic response due to cyclic load remain dominant (Fig. 4). When the time response is transformed to the frequency domain, the superimposed frequency response remains the same from the beginning to the end of the average, in which the cyclic load component is dominant and covers up the response due to the impact component (Fig. 5). In this case, only the superimposed frequency response is smoothed where the noises are diminished. The dominant peak cannot be diminished after 30 averages even when ISTA is used. From Table 1, the frequency response amplitude improvement of less

than 1% even after 30 averages shows that it is not efficient in eliminating the cyclic load component when the phase is consistent with every impact applied. This quantitative assessment also shows that there is little correlation between averaged and benchmarked frequency responses. In short, the phase angle with respect to impact is an important parameter in ISMA.

4.1.2 Inconsistent phase condition

In another simulation, impacts are designed by ensuring that the phase angles of the dominant periodic responses of the cyclic load with respect to impact are not consistent in every time record window block. Fig. 6a shows the responses generated when each time block acquisition is triggered by the impact at the beginning of an average. Superimposed responses are dominant because of the dominance of the periodic response due to cyclic load in the beginning when ISTA is to take place. When all of these time blocks are averaged in the time domain, the averaged time block (Fig. 6b) reveals that the response due to cyclic load is filtered out, maintaining the response due to impact after taking five averages. The averaged superimposed responses are identical with the benchmarked response due to impact. Note that there is still some random ambient noise as the number of averages used is relatively small for removing all the noises. Meanwhile, in the frequency domain, in the beginning of averaging, the cyclic
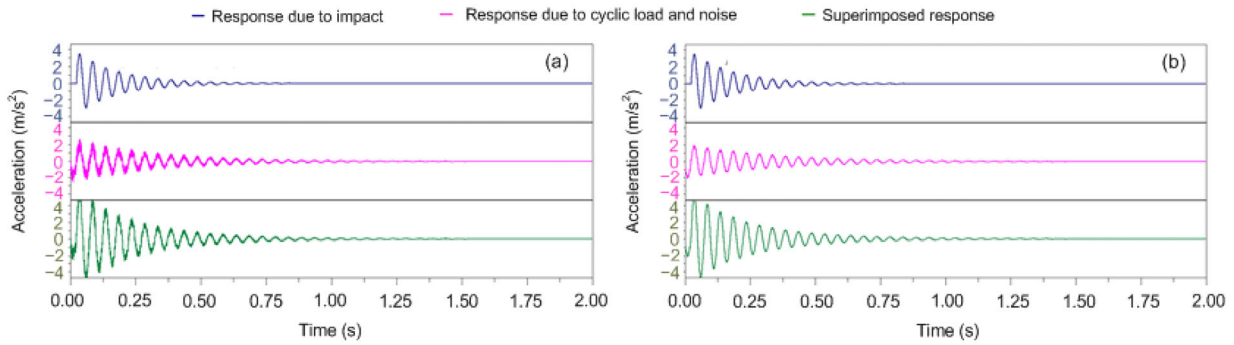

Fig. 4 Time responses at 20 Hz for consistent phase condition (for the references to color in this figure legend, the reader is referred to the web version of this article): (a) one average; (b) thirty averages with less than 1% improvement
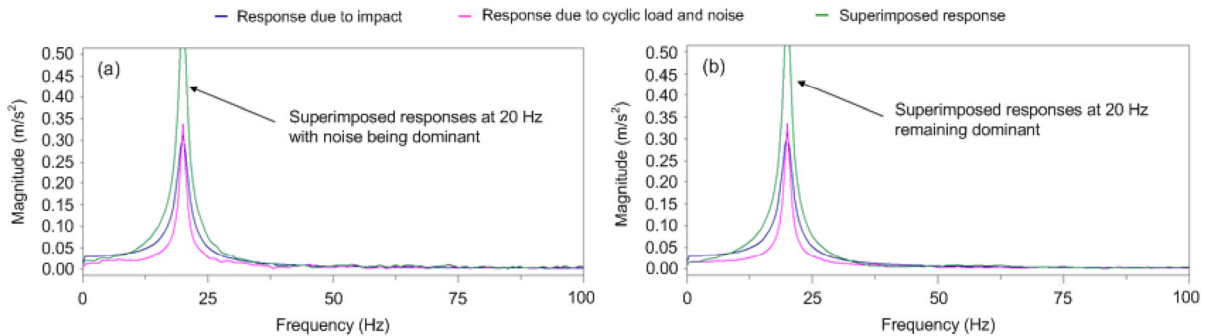

Fig. 5 Frequency responses for consistent phase condition (for the references to color in this figure legend, the reader is referred to the web version of this article): (a) one average; (b) thirty averages with less than 1% improvement

Table 1 Closeness of averaged superimposed frequency response to the benchmarked frequency response

Number of averages	Amplitude difference at 20 Hz (m/s^2)		Improvement (%)	
	Consistent phase	Inconsistent phase	Consistent phase	Inconsistent phase
1	0.33 813	0.17 426	−	−
5	0.33 712	0.00 265	0.30	98.48
30	0.33 596	0.00 212	0.64	98.78

load and noise components are dominant and they cover up the response due to the impact component (Fig. 7). After taking just five averages, the cyclic load and noise components are totally eliminated, leaving a smooth superimposed frequency response which is identical to the benchmarked frequency response generated purely by impact. The non-synchronous response components which contain even the same frequency as the component of the response due to impact are diminished when the phase is not consistent with respect to every impact signature.

The quantitative assessment in Table 1 shows 98.48% of improvement (i.e., reduction in frequency response amplitude at 20 Hz) by eliminating the non-synchronous components after taking five averages. The frequency response after five averages shows very good correlation with the benchmarked result. Even if the phase angle of the response due to cyclic load with every impact applied remains inconsistent after 30 averages, the improvement of frequency

response amplitude remains, i.e., 98.78%, and the averaged superimposed frequency response also remains identical with the benchmarked response due to impact.

4.2 Experimental modal testing

4.2.1 Scenario 1: consistent phase condition for all impacts

It is worth mentioning that although the possibility that a consistent phase condition occurs between the response due to impact and the response due to cyclic load is small, it is not totally impossible in modal testing using an impact hammer. Lack of knowledge and control of the impact with respect to the phase angle of the cyclic load is one of the limitations when carrying out ISMA using an impact hammer. Fig. 8 shows four responses due to impacts from modal testing for the first modal testing. It is observed that at the 100 pre-trigger samples phase position, the phases of the four responses due to impacts are consistent with the phase of the response
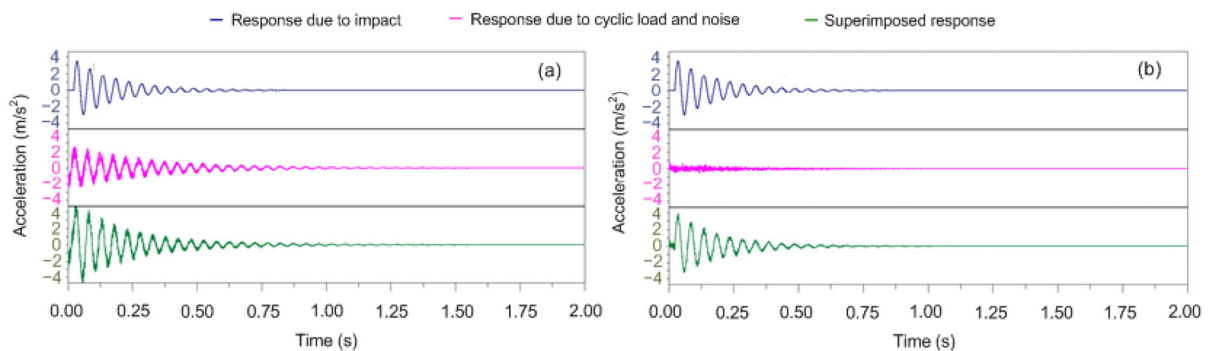

Fig. 6 Time responses at 20 Hz for inconsistent phase condition (for the references to color in this figure legend, the reader is referred to the web version of this article): (a) one average; (b) five averages with 98.48% improvement
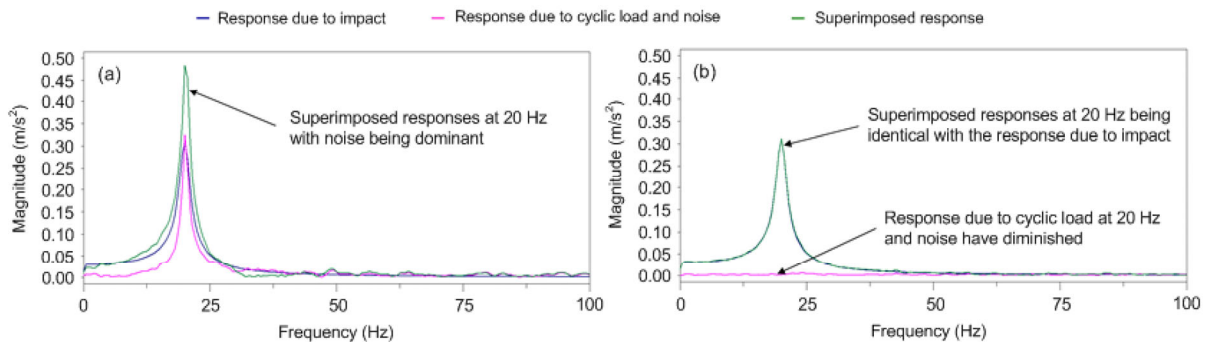

Fig. 7 Frequency responses for inconsistent phase condition (for the references to color in this figure legend, the reader is referred to the web version of this article): (a) one average; (b) five averages with 98.48% improvement

due to the cyclic load in every impact applied. In FRF estimation in Fig. 9, it is observed that the harmonic component at 20 Hz is not filtered out even when ISTA is used. The percentage differences for the frequency response amplitude between the benchmark and the consistent phase condition at the first and second natural peaks are large, i.e., 66.37% and 95.29% at the first and second natural peaks (Table 2). From Table 3, frequency response amplitude improvements of less than 5% even after four

averages at the first, the second natural peaks, and the first harmonic at 20 Hz show that it is not efficient in eliminating the cyclic load component when the phase is consistent with every impact applied.

4.2.2 Scenario 2: consistent phase condition for certain impacts

A more common scenario obtained when performing modal testing using a manual impact hammer on an operating system is presented in scenario 2. For scenario 2, it is observed that only the third average is synchronized with the fourth average (Fig. 10). Qualitatively, a slight decrease of frequency
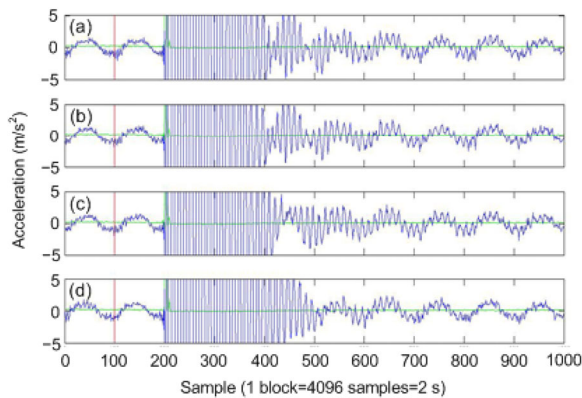

Fig. 8 Consistent phase condition at 100 pre-trigger samples phase position of response due to impact for scenario 1
(a) The first average; (b) The second average; (c) The third average; (d) The fourth average
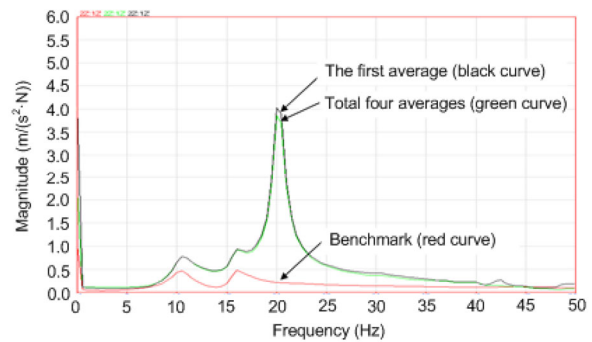

Fig. 9 FRF estimation for scenario 1 (for the references to color in this figure, the reader is referred to the web version of this article)

Table 2 Frequency response amplitude differences at the first and the second natural peaks between the benchmark and the consistent phase condition with four averages

Natural peak	Frequency response amplitude (m/(s²·N))			Percentage of difference (%)	
	Benchmark	Scenario 1	Scenario 2	Scenario 1	Scenario 2
First	0.458	0.762	0.759	66.37	65.72
Second	0.467	0.912	0.756	95.29	61.88

Table 3 Frequency response amplitude differences at the first, the second natural peaks, and 20 Hz between the first and the total four averages for the consistent phase condition

Frequency response amplitude (m/(s²·N))					
Number of averages	First natural peak		Second natural peak		20 Hz harmonic	
	Scenario 1	Scenario 2	Scenario 1	Scenario 2	Scenario 1	Scenario 2
1	0.761	0.844	0.930	0.825	4.030	4.030
4	0.762	0.759	0.912	0.756	3.830	2.680
Improvement (%)						
Number of averages	First natural peak		Second natural peak		20 Hz harmonic	
	Scenario 1	Scenario 2	Scenario 1	Scenario 2	Scenario 1	Scenario 2
1	−	−	−	−	−	−
4	−0.13	10.07	1.94	8.36	4.96	33.50

amplitude at 20 Hz harmonic frequency is expected. It is observable in Fig. 11 after performing four averages. The percentage differences for frequency response amplitude between the benchmark and the consistent phase condition at the first and the second natural peaks are large, i.e., 65.72% and 61.88% at the first and the second natural peaks, respectively (Table 2). From Table 3, the frequency response amplitude shows better improvement especially at 20 Hz, and records a value of 33.50% after four averages. The improvement in scenario 2 is due to the fact that only two averages are synchronized with the cyclic load component.

It should be noted from scenarios 1 and 2 that the number of impacts which have consistent phase with the cyclic load component can significantly influence the FRF estimation. Recall that the improvement of less than 5% at the harmonic frequency
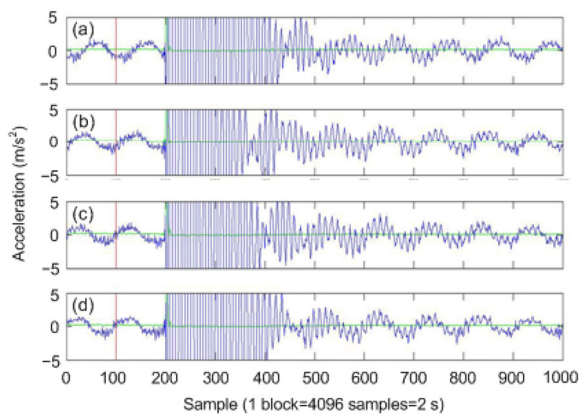
of 20 Hz for scenario 1 is because all the impacts are synchronized with the cyclic load component whereas scenario 2 can achieve an improvement of 33.50% because only two averages are synchronized with the cyclic load component, i.e., the third and the fourth averages. Generally, during the consistent phase condition, the response from the cyclic load will dominate and disturb the natural peak which is close to it, i.e., the second natural peak, so that it leads to improper identification of the mode.

4.2.3 Scenario 3: inconsistent phase condition for all impacts (ideal case: cyclic load components canceling each other out)

Fig. 12 shows four responses due to impacts from modal testing. It is observed that at the 100 pre-trigger samples phase position, the phases of the four responses due to impacts are inconsistent with the phase of the response due to cyclic load for every impact applied. In FRF estimation in Fig. 13, it is observed that the harmonic component at 20 Hz is filtered out when ISTA is used. The percentage differences for the frequency response amplitude between the benchmark and the inconsistent phase condition at the first and the second natural peaks are comparatively small, i.e., 23.80% and 10.49% at the first and the second natural peaks, respectively (Table 4). The quantitative assessment in Table 5 shows 38.97%, 54.91%, and 95.22% of improvements in frequency response amplitude at the first, the second natural peaks, and the first harmonic at 20 Hz by eliminating the non-synchronous components after taking four averages. The excellent improvement in the result is due to the fact that the cyclic load components cancel each other out during ISTA for (1) the first and the third averages and (2) the second and the fourth averages, leaving behind the desired response due to impact (Ong *et al.*, 2015).

4.2.4 Scenario 4: inconsistent phase condition for all impacts

Scenario 3 is an ideal case, and a more relevant condition commonly achieved by a manual impact hammer (i.e., scenario 4) is presented in this subsection. As shown in Fig. 14, at the 100 pre-trigger samples phase position, the phase of the response due to impacts is inconsistent with the phase of responses due to the cyclic load component. Qualitatively,

Fig. 10 Consistent phase condition at 100 pre-trigger samples phase position of response due to impact for scenario 2
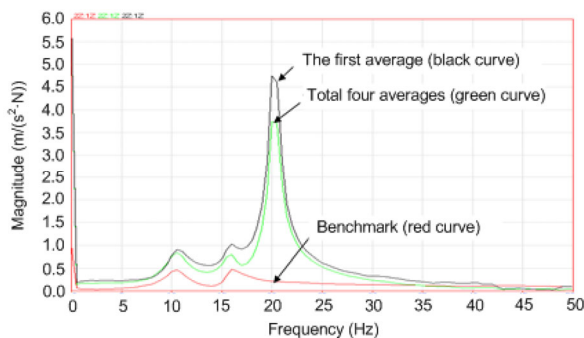(a) The first average; (b) The second average; (c) The third average; (d) The fourth average

Fig. 11 FRF estimation for scenario 2 (for the references to color in this figure, the reader is referred to the web version of this article)

an obvious decrease of frequency amplitude at the 20 Hz harmonic frequency can be seen in Fig. 15. It is observed that the percentage differences for the frequency response amplitude between the benchmark and the inconsistent phase condition at the first and the second natural peaks are slightly higher than that in scenario 3 (Table 4). From Table 5, the frequency response amplitude also shows better improvement compared to the consistent phase condition especially at 20 Hz, and records a value of 74.75% after four averages. However, the cyclic load

component is not totally filtered out in this case as the number of averages used is very small. It is believed that high number of averages which satisfy the inconsistent phase condition requirement would yield a better FRF estimation. Also, it is worth mentioning that the second natural peak experiences a higher percentage of improvement for scenarios 3 and 4 compared to the first natural peak as this mode is closer to the harmonic frequency of 20 Hz.

Recall that the percentage of improvement at a harmonic frequency of 20 Hz is higher in scenario 3
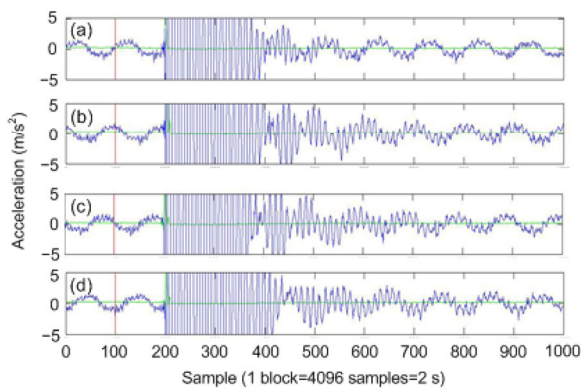

Fig. 12 Inconsistent phase condition at 100 pre-trigger samples phase position of response due to impact for scenario 3
(a) The first average; (b) The second average; (c) The third average; (d) The fourth average
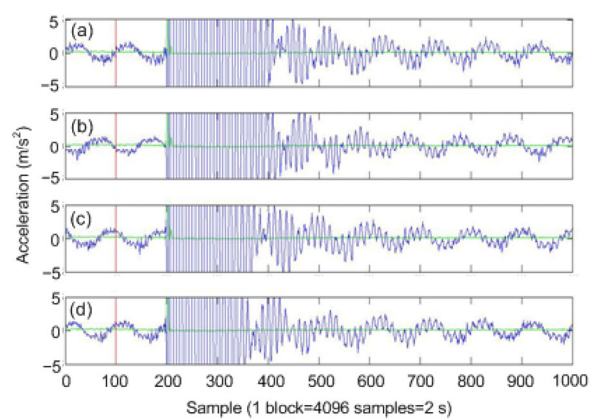

Fig. 14 Inconsistent phase condition at 100 pre-trigger samples phase position of response due to impact for scenario 4
(a) The first average; (b) The second average; (c) The third average; (d) The fourth average
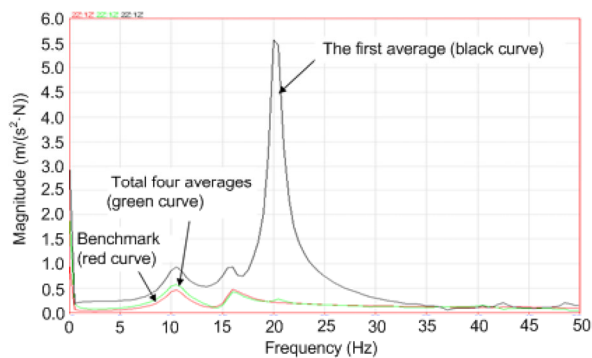

Fig. 13 FRF estimation for scenario 3 (for the references to color in this figure, the reader is referred to the web version of this article)
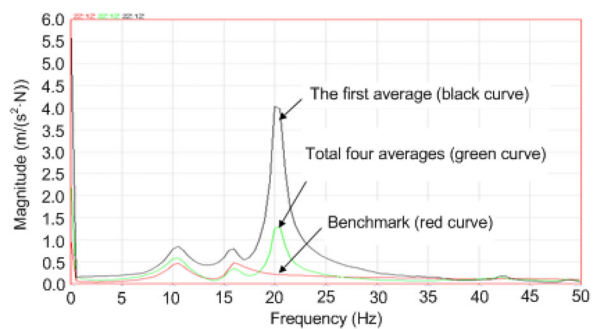

Fig. 15 FRF estimation for scenario 4 (for the references to color in this figure, the reader is referred to the web version of this article)

Table 4 Frequency response amplitude differences at the first and the second natural peaks between the benchmark and the inconsistent phase condition with four averages

Natural peak	Frequency response amplitude (m/(s²·N))			Percentage of difference (%)	
	Benchmark	Scenario 3	Scenario 4	Scenario 3	Scenario 4
First	0.458	0.567	0.578	23.80	26.20
Second	0.467	0.418	0.336	10.49	28.05

Table 5 Frequency response amplitude differences at the first, the second natural peaks, and 20 Hz between the first and the total four averages for the inconsistent phase condition

Frequency response amplitude (m/(s²·N))						
Number of averages	First natural peak		Second natural peak		20 Hz harmonic	
	Scenario 3	Scenario 4	Scenario 3	Scenario 4	Scenario 3	Scenario 4
1	0.929	0.839	0.927	0.784	5.570	4.040
4	0.567	0.578	0.418	0.336	0.266	1.300
Improvement (%)						
Number of averages	First natural peak		Second natural peak		20 Hz harmonic	
	Scenario 3	Scenario 4	Scenario 3	Scenario 42	Scenario 3	Scenario 4
1	–	–	–	–	–	–
4	38.97	28.25	54.91	49.49	95.22	74.75

compared to scenario 4, although both scenarios satisfy the condition of inconsistent phase between the response due to impact and the response due to cyclic load component. However, scenario 3 presents an additional benefit in that the cyclic load components tend to cancel each other out during ISTA, leaving behind the desired response due to impact. Nevertheless, both scenarios indicate the importance of the phase synchronization effect, i.e., inconsistent phase condition, in modal testing during operation with the minimum number of averages to eliminate the unaccounted force components.

5 Conclusions

The study on phase synchronization effect in ISMA using virtual instrument simulation and experimental modal testing has demonstrated the importance of phase angle with respect to impact in determination of dynamic characteristics. Synchronization of phases between impacts and the periodic response of the cyclic load should be avoided to enhance the effectiveness of ISMA. A small number of averages are sufficient to eliminate the non-synchronous components with 98.48% (simulation), 74.75% (scenario 4), and 95.22% (scenario 3) of improvement when every impact applied is not consistent with the phase angles of periodic response due to cyclic load.

Also, an improvement of 95.22% in scenario 3 which is much higher than that in scenario 4 indicates that there is probably a relationship between the phase angle of the cyclic load component and the

impact applied. Thus, future work can be proposed to further investigate this relationship with the aid of a portable calibrated auto-impact excitation device.

References

Aenlle, M.L., Brincker, R., 2013. Modal scaling in operational modal analysis using a finite element model. *International Journal of Mechanical Sciences*, **76**:86-101.
http://dx.doi.org/10.1016/j.ijmecsci.2013.09.003

Bienert, J., Andersen, P., Aguirre, R.C., 2015. A harmonic peak reduction technique for operational modal analysis of rotating machinery. 6th International Operational Modal Analysis Conference, p.619-625.

Bodeux, J.B., Golinval, J.C., 2001. Application of ARMAV models to the identification and damage detection of mechanical and civil engineering structures. *Smart Materials and Structures*, **10**(3):479-489.
http://dx.doi.org/10.1088/0964-1726/10/3/309

Brincker, R., Ventura, C., 2015. Introduction to Operational Modal Analysis. Wiley, p.1-16.

Brincker, R., Zhang, L., Andersen, P., 2000. Modal identification from ambient responses using frequency domain decomposition. Proceedings of the 18th International Modal Analysis Conference, p.625-630.

Dilena, M., Morassi, A., 2004. Experimental modal analysis of steel concrete composite beams with partially damaged connection. *Journal of Vibration and Control*, **10**(6):897-913.
http://dx.doi.org/10.1177/1077546304041370

Ding, Y.L., Li, A.Q., 2008. Finite element model updating for the Runyang Cable-stayed Bridge tower using ambient vibration test results. *Advances in Structural Engineering*, **11**(3):323-335.
http://dx.doi.org/10.1260/136943308785082599

Ding, Y.L., Li, A.Q., Liu, T., 2008. Environmental variability study on the measured responses of Runyang Cable-stayed Bridge using wavelet packet analysis. *Science in*

China Series E: Technological Sciences, **51**(5):517-528.
http://dx.doi.org/10.1007/s11431-008-0043-7

Fayyadh, M.M., Razak, H.A., Ismail, Z., 2011. Combined modal parameters-based index for damage identification in a beamlike structure: theoretical development and verification. *Archives of Civil and Mechanical Engineering*, **11**(3):587-609.
http://dx.doi.org/10.1016/S1644-9665(12)60103-4

Garcia-Perez, A., Amezquita-Sanchez, J.P., Dominguez-Gonzalez, A., *et al.*, 2013. Fused empirical mode decomposition and wavelets for locating combined damage in a truss-type structure through vibration analysis. *Journal of Zhejiang University-SCIENCE A (Applied Physics & Engineering)*, **14**(9):615-630.
http://dx.doi.org/10.1631/jzus.A1300030

Guillaume, P., Verboven, P., Vanlanduit, S., 1998. Frequency-domain maximum likelihood identification of modal parameters with confidence intervals. Proceedings of the 23rd International Seminar on Modal Analysis, p.359-366.

Guo, J., Chen, Y., Sun, B.N., 2005. Experimental study of structural damage identification based on WPT and coupling NN. *Journal of Zhejiang University-SCIENCE A*, **6**(7):663-669.
http://dx.doi.org/10.1007/BF02856170

He, J., Fu, Z.F., 2001. Modal Analysis. Butterworth-Heinemann, UK, p.1-11.

Ismail, Z., 2012. Application of residuals from regression of experimental mode shapes to locate multiple crack damage in a simply supported reinforced concrete beam. *Measurement*, **45**(6):1455-1461.
http://dx.doi.org/10.1016/j.measurement.2012.03.006

Ismail, Z., Ibrahim, Z., Ong, A., *et al.*, 2012. Approach to reduce the limitations of modal identification in damage detection using limited field data for nondestructive structural health monitoring of a cable-stayed concrete bridge. *Journal of Bridge Engineering*, **17**(6):867-875.
http://dx.doi.org/10.1061/(Asce)Be.1943-5592.0000353

James, G.H., Carne, T.G., Lauffer, J.P., 1995. The natural excitation technique (NExT) for modal parameter extraction from operating structures. *International Journal of Analytical and Experimental Modal Analysis*, **10**(4):260-277.

Lardies, J., Larbi, N., 2001. Dynamic system parameter identification by stochastic realization methods. *Journal of Vibration and Control*, **7**(5):711-728.
http://dx.doi.org/10.1177/107754630100700506

Le, T.P., Argoul, P., 2015. Distinction between harmonic and structural components in ambient excitation tests using the time-frequency domain decomposition technique. *Mechanical Systems and Signal Processing*, **52-53**:29-45.
http://dx.doi.org/10.1016/j.ymssp.2014.07.008

Li, A.Q., Ding, Y.L., Wang, H., *et al.*, 2012. Analysis and assessment of bridge health monitoring mass data—progress in research/development of "Structural Health Monitoring". *Science China Technological Sciences*, **55**(8):2212-2224.
http://dx.doi.org/10.1007/s11431-012-4818-5

Li, Z.J., Li, A.Q., Zhang, J., 2010. Effect of boundary conditions on modal parameters of the Run Yang Suspension Bridge. *Smart Structures and Systems*, **6**(8):905-920.
http://dx.doi.org/10.12989/sss.2010.6.8.905

Magalhães, F., Cunha, A., Caetano, E., 2012. Vibration based structural health monitoring of an arch bridge: from automated OMA to damage detection. *Mechanical Systems and Signal Processing*, **28**:212-228.
http://dx.doi.org/10.1016/j.ymssp.2011.06.011

Maia, N.M.M., Silva, J.M.M., 1997. Theoretical and Experimental Modal Analysis. Research Studies Press, UK.

Ong, Z.C., Kor, M.A.M.A., Brandt, A., 2015. Experimental validation of phase synchronisation effects in optimising impact-synchronous time averaging. 6th International Operational Modal Analysis Conference, p.551-558.

Phillips, A.W., Allemang, R.J., 2003. An overview of MIMO-FRF excitation/averaging/processing techniques. *Journal of Sound and Vibration*, **262**(3):651-675.
http://dx.doi.org/10.1016/S0022-460x(03)00116-0

Rahman, A.G.A., Ong, Z.C., Ismail, Z., 2011a. Effectiveness of impact-synchronous time averaging in determination of dynamic characteristics of a rotor dynamic system. *Measurement*, **44**(1):34-45.
http://dx.doi.org/10.1016/j.measurement.2010.09.005

Rahman, A.G.A., Ong, Z.C., Ismail, Z., 2011b. Enhancement of coherence functions using time signals in modal analysis. *Measurement*, **44**(10):2112-2123.
http://dx.doi.org/10.1016/j.measurement.2011.08.003

Rahman, A.G.A., Ismail, Z., Noroozi, S., *et al.*, 2014. Enhancement of impact-synchronous modal analysis with number of averages. *Journal of Vibration and Control*, **20**(11):1645-1655.
http://dx.doi.org/10.1177/1077546312475147

Rossmann, S., 1999. Development of Force Controlled Modal Testing on a Rotor Supported by Magnetic Bearing. MS Thesis, The Imperial College of Science, Technology and Medicine, University of London, UK.

Timoshenko, S.P., Young, D.H., 1974. Vibration Problems in Engineering. John Wiley & Sons Inc.

van Overschee, P., de Moor, B., 1996. Subspace Identification for Linear Systems: Theory–Implementation–Applications. Springer US, USA.
http://dx.doi.org/10.1007/978-1-4613-0465-4

Wang, H., Zou, K.G., Li, A.Q., *et al.*, 2010a. Parameter effects on the dynamic characteristics of a super-long-span triple-tower suspension bridge. *Journal of Zhejiang University-SCIENCE A (Applied Physics & Engineering)*, **11**(5):305-316.
http://dx.doi.org/10.1631/jzus.A0900496

Wang, H., Li, A.Q., Li, J., 2010b. Progressive finite element model calibration of a long-span suspension bridge based on ambient vibration and static measurements.

Engineering Structures, **32**(9):2546-2556.
http://dx.doi.org/10.1016/j.engstruct.2010.04.028

Wang, H., Mao, J.X., Huang, J.H., *et al.*, 2016. Modal identification of Sutong cable-stayed bridge during typhoon Haikui using wavelet transform method. *Journal of Performance of Constructed Facilities*, **30**(5): 0000856.
http://dx.doi.org/10.1061/(asce)cf.1943-5509.0000856

Wong, K.Y., 2004. Instrumentation and health monitoring of cable-supported bridges. *Structural Control and Health Monitoring*, **11**(2):91-124.
http://dx.doi.org/10.1002/stc.33

中文概要

题　目： 相位同步对工况下模态测试的影响评估分析

目　的： 通过研究证明激励信号的相位信息对同步激励模态分析的重要性：当各激励信号的相位信息非一致时，采用较少次数的时间平均即可实现对非激励–响应信号的滤除。

创新点： 通过对比采用一致相位激励信号和非一致相位激励信号下的频率响应函数，证明了当各激励信号的相位信息非一致时，采用较少次数的时间平均足以实现对非激励-响应信号的滤除。

方　法： 基于非一致相位信号的同步激励模态分析法。

结　论： 基于同步激励时间平均技术，通过对比采用一致相位激励信号和非一致相位激励信号下的频率响应函数，证明了当各激励信号的相位信息非一致时，采用较少次数的时间平均足以实现对非激励-响应信号的滤除。在仿真试验中，非同步信号成分的滤除效果提升了 98.48%；模态分析试验中，滤除效果提升了 95.22%。

关键词： 实验模态分析；振动；同步激励模态分析；同步激励时间平均；模态试验；相位同步